Selective Hg(II) Detection in Aqueous Solution with Thiol Derivatized Fluoresceins

Elizabeth M. Nolan, **Maryann E. Racine**, and **Stephen J. Lippard**[*]
Department of Chemistry, Massachusetts Institute of Technology, Cambridge, MA 02139

Abstract

The syntheses and photophysical properties of MS2 and MS3, two asymmetrically derivatized fluorescein-based dyes designed for Hg(II) detection, are described. These sensors each contain a single pyridyl-amine-thiol metal-binding moiety, form 1:1 complexes with Hg(II), and exhibit selectivity for Hg(II) over other Group 12 metals, alkali and alkaline earth metals, and most divalent first-row transition metals. Both dyes display superior brightness ($\Phi \times \varepsilon$) and fluorescence enhancement following Hg(II) coordination in aqueous solution. At neutral pH, the fluorescence turn-on derives from greater brightness due to increased molar absorptivity. At higher pH, photoinduced electron transfer (PET) quenching of the free dye is enhanced, and the Hg(II)-induced turn-on also benefits from alleviation of this pathway. MS2 can detect ppb levels of Hg(II) in aqueous solution, demonstrating its ability to identify environmentally relevant concentrations of Hg(II).

Introduction

Facile, sensitive and reliable methods for detecting heavy metal ions are important for research in environmental science and toxicology. Concern about human exposure to mercury through a variety of routes that include fish consumption,[1-5] vaccination,[6,7] dental amalgams[8] and both the household[8,9] and workplace[10] environments suggests the need for new tools capable of detecting inorganic mercury in aqueous solution and in biological samples. Small molecule fluorescent chemosensors that selectively bind to and report on the target metal ion constitute one practical route toward this goal.[11-16]

The design of sensors that give fluorescence enhancement upon Hg(II) binding is an intriguing challenge since Hg(II), like many heavy elements, often causes fluorescence quenching.[17] Restricting such turn-on Hg(II) sensors to aqueous environments adds an additional dimension of complexity to this problem. A variety of small-molecule Hg(II) detection strategies that use fluorescence have been documented.[18-34] Nevertheless, many of these Hg(II) probes have one or more limitations, which include irreversibility, slow response, incompatibility with aqueous solution, low selectivity, and fluorescence quenching upon Hg(II) coordination. Recently, several Hg(II) sensors that exhibit fluorescence turn-on and compatibility with the aqueous milieu have been described and include a biaryl pyridine species linked to an argogel resin[35] and xanthene-based MF1.[32] Other reported Hg(II) detection strategies relying on fluorescence output include nanoparticles,[36,37] polymers,[38] and biomolecules.[39,40] A number of colorimetric[41-48] Hg(II) indicators have also been documented.

As part of an on-going investigation focused on the preparation and utilization of small molecule metal ion sensors, we reported sensors MS1[49] and MS4[50] (Figure 1), both of which give a positive fluorescence response to Hg(II) in aqueous solution. In the design of MS1, we

*To whom the correspondence should be addressed: lippard@mit.edu.

employed fluorescein as the reporting group because of its water solubility and excellent photophysical properties ($\Phi \sim 1$, high ε). Sensor MS4 uses the seminaphthofluorescein chromophore, which affords single-excitation dual-emission ratiometric Hg(II) detection. MS1 and MS4 contain one or more thioether moieties in their metal-binding unit, which confers selectivity for Hg(II) over Zn(II) and Cd(II). Given the high affinity of Hg(II) for soft sulfur donors, including thiols, we have expanded our MS sensor family to include thiol-derivatized fluoresceins. In this work, we describe the syntheses, photophysical characterization, and Hg (II) binding properties of chemosensors containing pyridyl-amine-thiol ligands. Sensors MS2 and MS3, depicted in Scheme 1, are selective for Hg(II) over its Group 12 congeners, exhibit fluorescence turn-on immediately following Hg(II) coordination in aqueous solution and are, to the best of our knowledge, the brightest fluorescent Hg(II) sensors to date.

Experimental

Reagents

Toluene and acetonitrile were purged with Ar and dried by passing through columns of Al_2O_3. Ethyl acetate was dried over 3 Å molecular sieves and anhydrous 1,2-dichloroethane (DCE) was purchased from Aldrich. The compounds isobutylene sulfide,[51]**2**, MEPAH,[52]**3**, MEPAHTr,[53]**5**, and 7′-chloro-4′-bromomethylfluorescein di-*tert*-butyldimethylsilyl ether, [54]**7**, were synthesized as previously described. Isobutylene oxide, used in the synthesis of **2**, was purchased from TCI America. All other reagents were obtained from Aldrich and used as received, with the exception of 2-(aminomethyl)pyridine, which was vacuum distilled immediately before use.

Methods

Merck F254 silica gel-60 plates, Merck F254 aluminum oxide-60 plates, and octadecyl-functionalized (reverse phase, RP18) silica gel plates were used for analytical thin layer chromatography. TLC plates were viewed with UV light or after developing with ninhydrin stain. Either Whatman silica gel-60 plates or EM Science RP-18 F254 plates of 1 mm thickness were used as the solid phase for preparative TLC. A Varian 300 MHz or a Varian 500 MHz spectrophometer operating at 283 K was used to obtain ^{1}H and ^{13}C NMR spectra, which were referenced to the solvent peaks. IR spectra were obtained by using an Avatar FTIR instrument. An Agilent 1100 Series LCMS was used to obtain low resolution electrospray ionizaiton mass (ESI) spectrometry. High resolution ESI spectrometry was performed by staff in the MIT Department of Chemistry Instrumentation Facility.

2-Methyl-1-[(pyridin-2-ylmethyl)amino]propane-2-thiol (4)

A portion (12.0 g, 111 mmol) of freshly distilled 2-aminomethylpyridine was dissolved in 40 mL of toluene and heated to reflux. Isobutylene sulfide (**2**, 5.0 g, 57 mmol) was dissolved in 60 mL of toluene and added dropwise to the refluxing solution over 4 h. The reaction was refluxed for an additional 24 h, cooled, and the solvent was removed in vacuo. Vacuum distillation yielded the purified product as a colorless oil (4.9 g, 21%). ^{1}H NMR (CDCl$_3$, 300 MHz) δ 1.35 (6H, s, C*H*$_3$), 2.00 (2H, s, br, N*H* and S*H*), 2.60 (2H, s, C*H*$_2$CS), 3.93 (2H, s, NC*H*$_2$), 7.10 (1H, m, py-*H*), 7.30 (1H, d, py-*H*), 7.59 (1H, td, py-*H*), 8.49 (1H, dq, py-*H*). ^{13}C NMR (CDCl$_3$, 300 MHz) δ 30.73, 45.46, 55.78, 63.16, 121.85, 122.03, 136.35, 149.13, 159.97. An alternative preparation, which requires excess isobutylene sulfide, and further characterization are available elsewhere.[55]

(2-Methyl-2-triphenylsulfanylpropyl)pyridin-2-ylmethylamine (6)

A portion (1.44 g, 5.54 mmol) of triphenylmethanol and **4** (1.08 g, 5.51 mmol) were combined in a dry round-bottom flask and 9 mL of TFA was added. The reaction became brown-red and

the triphenylmethanol slowly dissolved. The reaction was stirred at room temperature for 2 h. The TFA was then removed under reduced pressure to yield an orange-red viscous oil. The oil was dissolved in 100 mL of ether and partitioned with 100 mL of 1 M NaOH and the layers were separated. The ether layer was concentrated under reduced pressure to afford the crude product as an off-white oily solid. Chromatography on Al_2O_3 with a solvent gradient (3:1 to 2:1 hexanes/EtOAc with 1% ^{i}PrNH$_2$) gave the purified product as an off-white solid (1.52 g, 63%). TLC R_f = 0.43 (Al_2O_3, 3:1 hexanes/EtOAc); mp = 82-84 °C. ^{1}H NMR (CDCl$_3$, 300 MHz) δ 1.17 (6H, s, CH_3), 1.75 (2H, s, CH_2CS), 1.96 (1H, s, br, NH), 3.67 (2H, s, NCH_2), 7.06-7.33 (12H, m, Tr-H and py-H), 7.56 (1H, td, py-H), 7.66 (5H, m, Tr-H), 8.49 (1H, dd, py-H). ^{13}C NMR (CDCl$_3$, 125 MHz) δ 28.75, 52.58, 55.35, 59.23, 67.28, 121.58, 121.66, 126.33, 127.51, 129.81, 136.20, 145.20, 148.88, 160.46. FTIR (KBr, cm^{-1}) 3435 (s), 3348 (m), 3049(w), 3026 (w), 2993 (w), 2972 (w), 2959 (w), 2950 (w), 2905 (w), 2851 (w), 1642(w), 1625 (w), 1589 (m), 1567(m), 1486(m), 1473 (m), 1444 (s), 1424 (m), 1380 (w), 1359 (m), 1319 (w), 1284 (w), 1242 (w), 1209 (w), 1130 (m), 1083 (w), 1031 (m), 1002 (w), 994 (w), 984 (w), 761 (m), 745 (s), 737 s), 705 (s), 673 (w), 665 (w), 629 (m), 620 (m). HRMS (ESI) Calcd MH$^+$, 439.2202; Found, 439.2209.

2-(2-Chloro-6-hydroxy-3-oxo-5-{[pyridin-2-ylmethyl-(2-triphenylsulfanyl-ethyl)amino] methyl}-3*H*-xanthen-9-yl)benzoic acid (8, MS2Tr)

To 8 mL of MeCN were combined 7′-chloro-4′-bromomethylfluorescein di-*tert*-butyldimethylsilyl ether (**7**, 150 mg, 0.22 mmol), MEPAHTr (**5**, 91 mg, 0.22 mmol) and K$_2$CO$_3$ (300 mg, 2.17 mmol), and the mixture was stirred overnight at room temperature. An orange precipitate formed and the reaction was filtered. TLC analysis showed the product to be present in both the precipitate and the filtrate. Preparative TLC of the combined material on reverse phase silica gel (9:1 CHCl$_3$\MeOH) yielded the pure product as an orange solid (142 mg, 82%). ^{1}H NMR (CD$_2$Cl$_2$, 300 MHz) δ 2.48 (4H, m, CH_2CH_2S), 3.68 (2H, s, fl-CH_2N), 3.90 (2H, s, py-CH_2N), 6.50-6.58 (2H, m, fl-H), 6.78 (1H, s, fl-H), 6.88 (1H, s, fl-H), 7.15-7.37 (18H, m, Tr-H, py-H and fl-H), 7.63-7.72 (3H, m, fl-H and py-H), 8.02 (1H, d, fl-H), 8.51 (1H, d, py-H). FTIR (KBr, cm^{-1}) 3431 (s), 2922 (vs), 2852 (s), 1763 (m), 1581 (m), 1514 (w), 1489 (m), 1465 (m), 1444 (m), 1370 (w), 1259 (m), 1210 (m), 1150 (m), 1090 (m), 1012 (m), 873 (w), 743 (m), 700 (s), 617(m), 473 (w), 444 (w). HRMS (ESI) Calcd MH$^+$, 789.2184; Found, 789.2200.

2-(2-Chloro-6-hydroxy-5-{[(2-mercaptoethyl)pyridin-2-ylmethylamino]methyl}-3-oxo-3*H*-xanthen-9-yl)benzoic acid (10, MS2)

A portion (142 mg, 0.180 mmol) of **8** was dissolved in 5 mL of TFA and a few drops of Et$_3$SiH were added. A white precipitate formed. The mixture was washed with hexanes (4 × 5 mL) and the TFA was removed under reduced pressure. Preparative TLC of the dark residue on reverse phase silica gel (6:1 MeOH\0.1 N HCl) afforded the purified product as an orange-red solid (55 mg, 56%). TLC R_f = 0.25 (RP silica, 6:1 MeOH\0.1 N HCl); mp = 194–196 °C, dec. ^{1}H NMR (CD$_3$OD, 300 MHz) δ 1.28 (1H, s, SH), 2.92 (2H, m, CH_2CS), 3.27 (2H, m, NCH_2), 4.27-4.46 (4H, m, NCH_2), 6.56 (2H, m, fl-H), 6.64 (1H, d, fl-H), 6.93 (1H, d, fl-H), 7.21 (1H, d, fl-H), 7.34 (1H, t, py-H), 7.43 (1H, d, py-H), 7.70-7.83 (3H, m, fl-H and py-H), 8.03 (1H, d, fl-H), 8.50 (1H, d, py-H). FTIR (KBr, cm^{-1}) 3434 (vs), 3055 (w), 2958 (w), 2918 (w), 2851 (w), 1762 (s), 1627 (s), 1600(s), 1581 (s), 1514 (w), 1489 (s), 1464 (s), 1452 (s), 1430 (s), 1370 (m), 1283 (s), 1260 (s), 1215 (s), 1149 (m), 1090 (m), 1106 (m), 1065 (w), 1012 (w), 874 (w), 822 (w), 801 (w), 760 (w), 702 (w), 621 (w), 596 (w). HRMS (ESI) Calcd MH$^-$, 545.0938; Found, 545.0963.

2-(2-Chloro-6-hydroxy-5-{[(2-mercapto-2-methylpropyl)pyridin-2-ylmethyl-amino]methyl}-3-oxo-3*H*-xanthen-9-yl)benzoic acid (11, MS3)

To 10 mL of MeCN and 1 mL of CH_2Cl_2 were added 7′-chloro-4′-bromomethylfluorescein di-*tert*-butyldimethylsilyl ether (**7**, 201 mg, 0.293 mmol), **6** (133 mg, 0.303 mmol), and K_2CO_3 (300 mg, 2.17 mmol). The reaction was stirred at room temperature for 24 h and filtered. The filtrate was evaporated to yield a dark orange residue, **9**, which was carried on without purification. Crude **9** was dissolved in 5 mL of TFA to yield a deep red solution and several drops of Et_3SiH were added. A white precipitate formed and the solution turned bright orange. The mixture was washed with hexanes (5×6 mL) and the TFA was removed in vacuo. Preparative TLC on silica gel (1:1:1:1 n-butanol/acetic acid/water/ethanol) followed by preparative TLC on reverse phase silica gel (3:1 MeOH/0.1 N HCl) afforded MS3 as an orange solid (30 mg, 17%). TLC R_f = 0.23 (RP silica, 3:1 MeOH/0.1 N HCl); mp = 194-196 °C, dec. ^1H NMR (CD_3OD, 300 MHz) δ 1.28 (7H, m, C*H*$_3$ and S*H*), 3.30 (2H, m, C*H*$_2$CS) 4.31-4.45 (4H, m, NC*H*$_2$), 6.51 (2H, m, fl-*H*), 6.64 (1H, d, fl-*H*), 6.99 (1H, s, fl-*H*), 7.17 (1H, d, fl-*H*), 7.32-7.36 (2H, m, py-*H*), 7.70-7.79 (3H, m, fl-*H* and py-*H*), 8.02 (1H, d, fl-*H*), 8.40 (1H, d, py-*H*). FTIR (KBr, cm^{-1}) 3430 (vs), 2957 (w), 2918 (m), 2850 (w), 1764 (m), 1628 (s), 1611 (s), 1462 (m), 1452 (m), 1428 (m), 1370 (w), 1284 (m), 1255 (m), 1219 (w), 1151 (w), 1107 (w), 1090 (w), 1014 (w), 875 (w), 762 (w), 698 (w). HRMS (ESI) Calcd MH^+, 575.1402; Found, 575.1394.

General Spectroscopic Methods

All aqueous solutions were prepared with Millipore water (18.2 MΩ·cm at 25 °C) obtained from a Mili-Q Biocel purifier outfitted with a Quantum VX cartridge. PIPES, piperazine-*N,N*′-bis(2-ethanesulfonic acid), CHES, 2-(*N*-cyclohexylamino)ethanesulfonic acid, and CABS, 4-cyclohexylamino-1-butanesulfonic acid, buffers were purchased from Sigma and used as received. Puratonic grade KCl was purchased from Calbiochem. Anhydrous $HgCl_2$ (99.998%) was purchased from Aldrich and used to prepare 10 mM Hg(II) stock solutions in water. Aqueous solutions of Li(I), Na(I), Rb(I), Mg(II), Ca(II), Sr(II), Ba(II), Cr(III), Mn(II), Co(II), Ni(II), Zn(II) and Cd(II) were prepared from the chloride salts, solutions of Fe(II) were prepared from ferrous ammonium sulfate and argon-purged water immediately before use, and solutions of Cu(II) were prepared from copper(II) sulfate. With the exception of the pK_a titrations, measurements were made in buffered aqueous solution with 50 mM buffer and 100 mM KCl at pH 7 (PIPES buffer), pH 9 (CHES buffer) or pH 11 (CABS buffer). A starting solution consisting of 10 mM KOH, 100 mM KCl (pH ~12) was used for the pK_a titrations as described in the Fluorescence Spectroscopy section below. Stock solutions (1 mM) of MS2 and MS3 in DMSO were prepared, stored at −25 °C, and thawed in the dark before use. These stock solutions are stable for >12 months under these conditions judging by UV-vis and fluorescence spectroscopy. After dilution of this stock in the appropriate buffer, the resulting solutions contained 0.1% or 1% DMSO for fluorescence or absorption measurements, respectively. With the exception of the pK_a titrations, which were performed in duplicate, all manipulations were performed at least in triplicate and the averages are reported. All data were manipulated by using the KaleidaGraph software package.

Optical Absorption Spectroscopy

UV-visible spectra were collected on a Hewlett-Packard 8453 diode array spectrophotometer maintained at 25 °C ± 1 °C with a circulating water bath. Quartz cuvettes (Starna) with a 1-cm path length and 3.5-mL volume were used for all measurements. Job analyses and metal-binding titrations were conducted to determine the stoichiometry of the MS2 and MS3 mercury-bound complexes in solution. In a typical Job analysis, starting solutions of 10 μM dye and 10 μM $HgCl_2$ were used and the data were analyzed according to the standard equation $A^* = A_{obs} - \varepsilon_{lig}[lig]$, where ε_{lig} is the molar absorptivity at the wavelength of interest and lig refers

to the metal-free probe. For a typical metal-binding titration, 3 μL aliquots of a 1 mM Hg(II) solution were added to a 10 μM solution of dye. The absorbance changes were plotted against equivalents of Hg(II) in solution.

Fluorescence Spectroscopy

Fluorescence spectra were collected by using a Hitachi F-3010 spectrofluorimeter maintained at 25 °C ± 1 °C by a circulating water bath. Quartz cuvettes (Starna) with a 1-cm path length and 3.5-mL volume were used for all fluorescence measurements. Excitation and emission slit widths of 3 nm were used for data acquisition. Quantum yields were measured relative to fluorescein in 0.1 N NaOH ($\Phi = 0.95$).[56] The pH-dependent pK_a values were determined by adding aliquots of 6, 2, 1, 0.5 and 0.1 N HCl to a 1 μM solution of the sensor in 10 mM KOH, 100 mM KCl. The volume change for each pK_a experiment did not exceed 3%. The emission spectra were recorded at pH intervals of ~0.25 and the spectra were integrated, normalized and plotted against pH. The data were fit to the non-linear equation previously described.[57] Metal ion selectivity experiments were conducted as described for MS1.[49]

Results and Discussion

Syntheses of Sensors MS2 and MS3

Several small-molecule Hg(II) detectors that employ sulfur donors have been reported by our laboratory[49,50] and others.[22,30-34] These probes have sulfur-containing macrocycles,[31-34] thioether,[30,49,50] or thiourea groups[35] in the metal-binding units and generally exhibit good selectivity for Hg(II). Given the propensity of Hg(II) to bind thiols, we anticipated that incorporation of thiol donors into the metal-binding unit of a sensor would elicit both high selectivity and sensitivity for Hg(II).

The syntheses for MS2 and MS3 are illustrated in Scheme 1. MEPAHTr, **5**, was prepared according to a literature procedure.[53] Combination of **5** with the silyl protected bromomethyl fluorescein,[54] **7**, in the presence of excess K_2CO_3 and subsequent preparative TLC on reverse phase silica gel (9:1 $CHCl_3$/MeOH) afforded MS2Tr, **8**, in high yield (82%) as an orange solid. As observed in the reported synthesis of sensor ZS3,[58] the TBS protecting groups of **7** were unstable to these conditions, and deprotection occurred during the course of the reaction. The trityl protecting group was subsequently removed by drop-wise addition of Et_3SiH to a solution of **8** in TFA followed by washing with hexanes. Preparative TLC of the crude product on reverse phase silica gel (4.5:1 MeOH/0.1 N HCl) yielded pure MS2, **10**, as an orange solid in moderate yield (56%).

MS3 differs from MS2 by having *gem*-dimethyl substituents incorporated into the pyridyl-amine-thiol ligand. Compound **4** was prepared from isobutylene sulfide and 2-(aminomethyl)pyridine by analogy to the published procedure[52] for **3** and was obtained in moderate yield as a colorless oil following vacuum distillation. The thiol was protected with a trityl group and **6** was isolated as a white solid in 63% yield following work-up and chromatography on Al_2O_3 using a hexanes/EtOAc solvent gradient. The assembly of MS3 from **6** and **7** is analogous to that described above for MS2. During this procedure, however, intermediate **9** was not purified before deprotection of the thiol moiety. Pure MS3, **11**, was isolated as an orange-red solid in relatively low yield (17%) after purification by preparative TLC. Both MS2 and MS3 have a faint sulfurous odor and the purified sensors are stable for >12 months when stored in the dark at 4 °C as judged by absorption and fluorescence spectroscopy.

Spectroscopic Properties of MS2 and MS3

MS2 and MS3, shown in Scheme 1, were designed as turn-on photoinduced electron transfer (PET) sensors that utilize tertiary amines as the quenching unit. The generally accepted

mechanism for fluorescence turn-on in amine-based PET sensors involves fluorescence quenching of the free dye by PET through back-electron transfer from a nitrogen lone pair electron in the photoexcited state, followed by diminution of PET via coordination to a closed shell metal ion, which results in fluorescence enhancement.[12]

Table 1 summarizes the results from spectroscopic characterization of MS2 and MS3. These dyes each contain a pyridyl-amine-thiol ligand installed in the 4′ position of the fluorescein platform. Given the structural similarity between these two compounds, we anticipated that they would exhibit comparable photophysical properties. In all instances, the results met our expectations.

Unbound MS2 and MS3 show essentially identical pH-emission profiles, which are illustrated in Figure 2. The fluorescence of each probe is ~75% quenched at pH 12 and maximum fluorescence is reached at pH ~7. Two protonation events affect the fluorescence of MS2 (pK_a = 8.2, 4.6) and MS3 (pK_a = 8.0, 4.6). The pK_a ~8 transition is assigned to the tertiary nitrogen atom, protonation of which interferes with the PET quenching pathway and yields enhanced fluorescence at neutral pH. This assignment is based on comparison of the pK_a profiles of tertiary amine-based ZP dyes[57] and related compounds,[58] although we note that pK_a values for thiols could also fall in this range. Fluorescein itself displays pH-dependent fluorescence with quenched emission at low pH, and the pK_a of 4.6 observed in Figure 2 corresponds to fluorescein protonation and formation of a non-fluorescent species at acidic pH.

MS2 and MS3 have quantum yields of 0.28 and 0.27 and emission maxima at 526 and 525, respectively, at neutral pH (50 mM PIPES, 100 mM KCl) and in the presence of the metal ion scavenger of EDTA (Table 1). These values are approximately ~50% lower than that observed for the corresponding asymmetrical di(2-picolyl)amine-based sensor ($\Phi \sim 0.6$), which suggests that the thiol moiety also plays a role in quenching the fluorescein excited state. Addition of Hg(II) causes a ~1.5-fold (MS2) or ~2-fold (MS3) fluorescence enhancement and the emission spectra for both species red-shift to 531 nm (Figure 3). The absorption spectra also undergo red-shifts upon Hg(II) complexation. For MS2, a 5 nm shift is observed from 500 nm (ε = 62,000 $M^{-1}cm^{-1}$) to 505 nm (ε = 69,000 $M^{-1}cm^{-1}$). The optical absorption spectrum for MS3 exhibits a similar shift from 501 nm (ε = 51,000 $M^{-1}cm^{-1}$) to 507 nm (ε = 59,000 $M^{-1}cm^{-1}$) following Hg(II) binding. Since introduction of Hg(II) to a solution of MS2 or MS3 at pH 7 results in essentially no change in quantum yield for either species (MS2, Φ_{Hg} = 0.27; MS3, Φ_{Hg} = 0.28) while causing an increase in molar absorptivity, the resulting fluorescence enhancement is due exclusively to the absorption increase since brightness is ($\Phi \times \varepsilon$).

Although modest, the fluorescence enhancement observed for these sensors upon addition of Hg(II) was intriguing. The pK_a of ~8 for MS2 and MS3 suggests that proton-induced background fluorescence compromises Hg(II)-induced emission turn-on at neutral pH. Raising the solution pH to deprotonate the tertiary amine nitrogen atom should enhance PET quenching, lower the quantum efficiency of each free dye and result in greater fluorescence enhancement upon Hg(II) complexation. As anticipated, the quantum yield of free MS2 decreases substantially when the pH is raised to 9 (50 mM CHES, 100 mM KCl) or 11 (50 mM CABS, 100 mM KCl) with values of 0.10 and 0.07, respectively. A ~5-fold increase in integrated emission immediately results after addition of Hg(II) to MS2 in this pH regime (Figure S1, Supporting Information) and the quantum yield of the Hg(II) complex is 0.28 (pH 9) or 0.24 (pH 11). MS3 exhibits analogous behavior, as summarized in Table 1. Despite the relatively modest degree of turn-on at pH 7, the choice of tertiary amine as a PET switch and fluorescein as the reporting group achieves greater brightness ($\Phi \times \varepsilon$) upon Hg(II) coordination than that observed for the aniline-derivatized members of the MS family (Figure 1) and Hg(II) sensors

reported by others. To the best of our knowledge, MS2 and MS3 are the brightest water-soluble Hg(II) sensors to date.

Metal Binding Studies of MS2 and MS3

Asymmetrical MS2 and MS3 were designed for 1:1 metal ion complexation and the metal-binding properties of these probes were investigated by UV-visible and fluorescence spectroscopies. Job plots for the addition of Hg(II) to solutions of MS2 and MS3 are given as Supporting Information (Figure S2). The inflection points at 0.5 indicate the formation of 1:1 MS2:Hg(II) and MS3:Hg(II) complexes in aqueous solution. Metal-binding titrations reveal a break at 1 equiv of Hg(II), providing further evidence for 1:1 binding stiochiometry (Figure 4). At pH 7 (50 mM PIPES, 100 mM KCl), the absorbance difference spectrum for the addition of Hg(II) to MS2 shows a decrease at 483 nm and increases at ca. 300 and 512 nm. The difference spectrum for MS3 is similar (decrease at 482 nm; increases at ca. 300 and 510 nm). Comparable absorption changes are observed for Hg(II) binding at high pH. For instance, at pH 11 (50 mM CABS, 100 mM KCl) Hg(II) binding to MS2 results in an absorbance increase at 510 nm and a decrease at 490 nm (Figure 4). The absorbance changes at ca. 500 nm are attributed to perturbation of the fluorescein $\pi\pi^*$ transition upon Hg(II) coordination and the increase at ca. 300 nm to $RS^- \rightarrow Hg(II)$ charge transfer bands.[59,60]

Sensors MS2 and MS3 both show diminished fluorescence turn-on following Hg(II) binding at neutral pH in the absence of chloride ion, as previously observed for MS1[49] and MS4.[50] For instance, at neutral pH (50 mM PIPES, 1000 mM KX, X = OAc^-, F^-, NO_3^-), only negligible (KOAc, KF) or no (KNO_3) fluorescence enhancement occurs following Hg(II) binding to MS2 (Figure S3). The presence of chloride ion has no effect on the emission profile of the free dyes, suggesting that a Hg—Cl bond or ion pairing causes the chloride-dependent fluorescence enhancement. Results obtained from low resolution ESI mass spectrometric analyses of solutions of MS2 and Hg(II) with added chloride ion support this notion. When a methanolic solution of equimolar MS2 and Hg(II) is treated with aqueous KCl, two new intense peaks with m/z of 780.6 and 816.6 are observed in the negative ion mode mass spectrum (Figure S4). The former m/z ratio corresponds to the monochloro adduct, [MS2+Hg+Cl-2H] (calcd. 781.0), and the latter to the dichloro species [MS2+Hg+2Cl-H] (calcd. 817.0). Although the precise nature of these chloride-containing complexes cannot be ascertained from this experiment, the data clearly reveal that the MS2:Hg(II) complex associates with one or more chloride ions in solution. This association, in turn, modulates the fluorescence emission of the Hg(II) complex.

Fluorescence spectroscopy was used to determine an EC_{50} value, the concentration of Hg(II) required for 50% of the total fluorescence enhancement at [MS] = 1 μM, for Hg(II) binding to MS2 and MS3 (Figure S1). Essentially complete turn-on (~96%) results upon addition of 1 equiv of Hg(II) to a solution of MS2, and the EC_{50} of MS2 for Hg(II) is 384 nM. Addition of 1 equiv of Hg(II) to MS3 results in ~34% turn-on and maximum fluorescence is reached with ~6 equiv of Hg(II) in solution. The EC_{50} for MS3 for Hg(II) is 1.6 μM, indicating that *gem*-dimethyl susbtituents adjacent to the thiol donor decrease the binding affinity. These values may be compared to the EC_{50} value of 410 nM for sensor MS1 (1 μM, pH 7).[49]

Achieving high selectivity for the analyte of interest over a complex background of potentially competing species is a challenge in sensor development. Figure 5 illustrates the fluorescence response of MS3 to Hg(II) in the presence of alkali and alkaline earth metals found in natural waters,[61] select divalent first-row transition metals, and Zn(II) and Cd(II). A background of Group 1 and 2 metals does interfere with Hg(II) coordination and subsequent fluorescence turn-on. Neither Cr(III) nor Pb(II) prevent the Hg(II)-induced fluorescence enhancement. MS3 is selective for Hg(II) over the open-shell divalent first-row transition metals Mn(II), Fe(II) and Co(II). MS3 preferentially binds Ni(II) and Cu(II) over Hg(II) at neutral pH, as observed for sensor MS4[50], which also employs one sulfur and one pyridyl nitrogen donor atom. The

selectivity of MS2 for Hg(II) is generally similar, although slightly less fluorescence enhancement occurs upon addition of Hg(II) to solutions of MS2 and Co(II) (Figure S5). The preference of sensors MS1-4 for Cu(II) is not surprising given the N_2SO donor set and the observation that sulfur-containing ligands exhibit high affinity for metals in the "copper triangle" of the periodic table.[62] Like MS1 and MS4, sensors MS2 and MS3 both display greater affinity for Hg(II) than its Group 12 congeners Zn(II) and Cd(II). The positive fluorescence responses of MS2 and MS3 are Hg(II)-specific (Figure 5).

Reversibility is a criterion in sensor development since the ability to regenerate the free sensor is important for practical applications. During our investigation of anion effects, we observed that MS2 and MS3 do not coordinate Hg(II) in buffer containing 100 mM KI (50 mM PIPES, 100 mM KI, pH 7). Optical absorption spectroscopy showed that addition of Hg(II) to solutions of the sensors in this buffer resulted in no change in the chromophore absorption band centered at 500 nm and the formation of intense absorption bands centered at 265 and 321 nm attributed to $[HgI_4]^{2-}$ (Figure S6).[63,64] This finding and a recent report that Hg(II) complexation to a solid-state colorimetric Hg(II) sensor was reversed by washing with KI[46] motivated us to use KI to achieve reversible Hg(II) binding with MS2. Optical absorption spectroscopy shows that addition of excess KI to solutions of the MS2:Hg(II) complex causes an immediate blue shift in the fluorescein $\pi\pi^*$ transition from 505 to 500 nm with a concomitant intensity decrease, consistent with Hg(II) release. As anticipated, formation of new bands in the 260-320 nm region signaled formation of $[HgI_4]^{2-}$ (Figure S6).

The EPA mandated upper-limit of allowable inorganic mercury in drinking water is 2 ppb.[3] A fluorescence change of 15.3% ± 5% in MS2 (500 nM) occurs in the presence of 2 ppb Hg(II) (50 mM CABS, 100 mM KCl, pH 11), demonstrating that MS2 can detect environmentally relevant concentrations of Hg(II).

Summary

MS2 and MS3, two water-soluble, fluorescein-based Hg(II) sensors that each contain a pyridyl-amine-thiol ligand were prepared and characterized. These probes afford Hg(II)-selective fluorescence enhancement in aqueous solution at neutral pH and EC_{50} values for Hg(II) in the mid-nM to low μM range. MS2 and MS3 bind Hg(II) over Zn(II), Cd(II), Mn(II), Fe(II), Co(II), Cr(III), Pb(II) and millimolar concentrations of various alkali and alkaline earth metals. The choice of tertiary amine nitrogen atoms as the PET switch yields fluorescein-based sensors and Hg(II) complexes with superior brightness ($\Phi \times \varepsilon$) compared to aniline-containing MS1 and other reported water-soluble Hg(II) sensors. The MS2 and MS3 sensors may be useful for applications in toxicology and environmental sciences.

Supplementary Material

Refer to Web version on PubMed Central for supplementary material.

References

1. Boening DW. Chemosphere 2000;40:1335–1351. [PubMed: 10789973]

2. Renzoni A, Zino F, Franchi E. Environ Res 1998;77:68–72. [PubMed: 9600797]

3. EPA Fact Sheet EPA-823-F-01-011. EPA, Office of Water; Washington, DC: 2001. Mercury Update: Impact on Fish Advisories.

4. Nendza M, Herbst T, Kussatz C, Gies A. Chemosphere 1997;35:1875–1885. [PubMed: 9353909]

5. Harris HH, Pickering IJ, George GN. Science 2003;301:1203. [PubMed: 12947190]

6. Pichichero ME, Cernichiari E, Lopreiato J, Treanor J. Lancet 2002;360:1737–1741. [PubMed: 12480426]

7. Magos L. J Applied Toxicol 2001;21:1–5. [PubMed: 11180274]

8. Clarkson TW, Magos L, Myers GJ. New Eng J Med 2003;349:1731–1737. [PubMed: 14585942]

9. Forman J, Moline J, Cernichiari E, Sayegh S, Torres JC, Landrigan MM, Hudson J, Adel HN, Landrigan PJ. Environ Heatlh Perspect 2000;108:575–577.

10. Malm O. Environ Res 1998;77:73–78. [PubMed: 9600798]

11. Czarnik AW. Acc Chem Res 1994;27:302–308.

12. de Silva AP, Guarante HQN, Gunnlaugsson T, Huxley AJM, McCoy CP, Rademacher JT, Rice TE. Chem Rev 1997;97:1515–1566. [PubMed: 11851458]

13. de Silva AP, Fox DB, Huxley AJM, Moody TS. Coor Chem Rev 2000;205:41–57.

14. Prodi L. New J Chem 2005;29:20–31.

15. Prodi L, Bolletta F, Montalti M, Zaccheroni N. Coor Chem Rev 2000;205:59–83.

16. Callan JF, de Silva AP, Magri DC. Tetrahedron 2005;61:8551–8588.

17. Masuhara H, Shioyama H, Saito T, Hamada K, Yasoshima S, Mataga N. J Phys Chem 1984;88:5868–5873.

18. Chae MY, Czarnik AW. J Am Chem Soc 1992;114:9704–9705.

19. Hennrich G, Walther W, Resch-Genger U, Sonnenschein H. Inorg Chem 2001;40:641–644. [PubMed: 11225105]

20. Metivier R, Leray I, Valeur B. Chem Eur J 2004;10:4480–4490.

21. Ros-Lis JV, Marcos MD, Martinez - Manez R, Rurack K, Soto J. Angew Chem Int Ed 2005;44:4405–4407.

22. Dickerson TJ, Reed NN, La Clair JJ, Janda KD. J Am Chem Soc 2004;126:16582–16586. [PubMed: 15600364]

23. Guo X, Qian X, Jia L. J Am Chem Soc 2004;126:2272–2273. [PubMed: 14982408]

24. Caballero A, Martinez R, Lloveras V, Ratera I, Vidal-Gancedo J, Wurst K, Tarraga A, Molina P, Veciana J. J Am Chem Soc 2005;127:15666–15667. [PubMed: 16277484]

25. Chen QY, Chen CF. Tetrahedron Lett 2005;46:165–168.

26. Moon SY, Youn NJ, Park SM, Chang SK. J Org Chem 2005;70:2394–2397. [PubMed: 15760241]

27. Zhang G, Zhang D, Yin S, Yang X, Shuai Z, Zhu D. Chem Commun 2005:2161–2163.

28. Liu B, Tian H. Chem Commun 2005:3156–3158.

29. Yang YK, Yook KJ, Tae J. J Am Chem Soc 2005;127ASAP

30. Sakamoto H, Ishikawa J, Nakao S, Wada H. Chem Commun 2001:2395–2396.

31. Descalzo AB, Martinez-Manez R, Radeglia R, Rurack K, Soto J. J Am Chem Soc 2003;125:3418–3419. [PubMed: 12643689]

32. Yoon S, Albers AE, Wong AP, Chang CJ. J Am Chem Soc 2005;127:16030–16031. [PubMed: 16287282]

33. Rurack K, Kollmannsberger M, Resch-Genger U, Daub J. J Am Chem Soc 2000;122:968–969.

34. Rurack K, Resch-Genger U, Bricks JL, Spieles M. Chem Commun 2000:2103–2104.

35. Mello JV, Finney NS. J Am Chem Soc 2005;127:10124–10125. [PubMed: 16028896]

36. Chen B, Yu Y, Zhou Z, Zhong P. Chem Lett 2004;33:1608–1609.

37. Zhu C, Li L, Fang F, Chen J, Wu Y. Chem Lett 2005;34:898–899.

38. Fan LJ, Zhang Y, Jones WE. Macromolecules 2005;38:2844–2849.

39. Ono A, Togashi H. Angew Chem Int Ed 2004;43:4300–4302.

40. Chen P, He C. J Am Chem Soc 2004;126:728–729. [PubMed: 14733542]

41. Brummer O, La Clair JJ, Janda KD. Org Lett 1999;1:415–418.

42. Sancenon F, Martinez - Manez R, Soto J. Chem Commun 2001:2262–2263.

43. Sancenon F, Martinez - Manez R, Soto J. Tetrahedron Lett 2001;42:4321–4323.

44. Choi MJ, Kim MY, Chang SK. Chem Commun 2001:1664–1665.

45. Palomares E, Vilar R, Durrant JR. Chem Commun 2004:362–363.

46. Coronado E, Galan-Mascaros JR, Marti-Gastaldo C, Palomares E, Durrant JR, Vilar R, Gratzel M, Nazeeruddin MK. J Am Chem Soc 2005;127:12351–12356. [PubMed: 16131215]

47. Ros-Lis JV, Martinez - Manez R, Rurack K, Sancenon F, Soto J, Spieles M. Inorg Chem 2004;43:5183–5185. [PubMed: 15310190]

48. Balaji T, Sasidharan M, Matsunaga H. Analyst 2005;130:1162–1167. [PubMed: 16021215]

49. Nolan EM, Lippard SJ. J Am Chem Soc 2003;125:14270–14271. [PubMed: 14624563]

50. Nolan EM, Lippard SJ. J Mat Chem 2005;15:2778–2783.

51. Snyder HR, Stewart JM, Ziegler JB. J Am Chem Soc 1947;69:2672–2674.

52. Brand U, Vahrenkamp H. Inorg Chem 1995;34:3285–3293.

53. Kramer DJ, Davison A, Davis WM, Jones AG. Inorg Chem 2002;41:6181–6183. [PubMed: 12444754]

54. Burdette SC, Frederickson CJ, Bu W, Lippard SJ. J Am Chem Soc 2003;125:1778–1787. [PubMed: 12580603]

55. Brand U, Vahrenkamp H. Inorg Chim Acta 2000;308:97–102.

56. Brannon JH, Magde D. J Phys Chem 1978;82:705–709.

57. Burdette SC, Walkup GK, Spingler B, Tsien RY, Lippard SJ. J Am Chem Soc 2001;123:7831–7841. [PubMed: 11493056]

58. Nolan EM, Lippard SJ. Inorg Chem 2004;43:8310–8317. [PubMed: 15606177]

59. Watton SP, Wright JG, MacDonnell FM, Bryson JW, Sabat M, O'Halloran TV. J Am Chem Soc 1990;112:2824–2826.

60. Fleissner G, Kozlowski PM, Vargek M, Bryson JW, O'Halloran TV, Spiro TG. Inorg Chem 1999;38:3523–3528. [PubMed: 11671099]

61. Drever, JI. The Geochemistry of Natural Waters: Surface and Groundwater Environments. 3rd. Prentice Hall; Upper Saddle River, NH: 1997.

62. Cooper TH, Mayer MJ, Leung KH, Ochrymowycz LA, Rorabacher DB. Inorg Chem 1992;31:3796–3804.

63. Griffiths TR, Symons MCR. J Chem Soc Trans Farady Soc 1960;56:1752–1760.

64. Griffiths TR, Anderson RA. Can J Chem 1991;69:451–457.

Figure 1.
Mercury Sensors 1 (MS1) and 4 (MS4). MS1 gives a fluorescence enhancement upon addition of Hg(II) at neutral pH (ref. 49). MS4 provides a ratiometric response to Hg(II) at pH 8 (ref. 50).
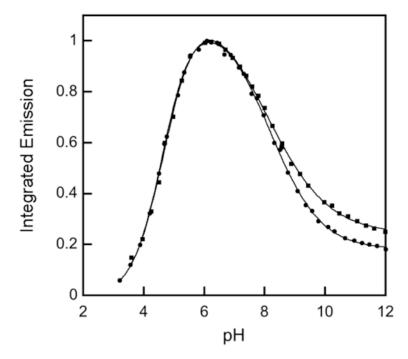
Figure 2.
Fluorescence dependence on pH for free MS2 (circles) and MS3 (squares). A 1 μM solution
of each dye was prepared and the emission spectrum was taken. Aliquots of 6 2, 1, 0.5 and 0.1
N HCl were added to achieve pH changes of ~0.25 units and the emission spectrum was
recorded at each interval. The emission was integrated from 500 – 650 nm (MS2) or from 450
– 650 nm (MS3), normalized and plotted against pH. Excitation was provided at 498 nm. Two
protonation events affect the fluorescence of MS2 and MS3 with $pK_{a1} = 8.0$ (MS2) or 8.2
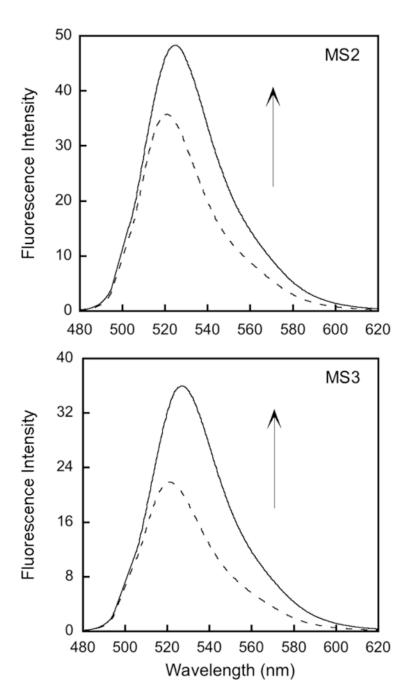(MS3) and $pK_{a2} = 4.6$.

Figure 3.
The fluorescence response of 1 μM MS2 (top) and MS3 (bottom) to 50 equiv of Hg(II) at pH 7 (50 mM PIPES, 100 mM KCl). Dotted line: MS2 or MS3; solid line: +Hg(II). Excitation was provided at 500 nm for MS2 and at 504 nm for MS3.
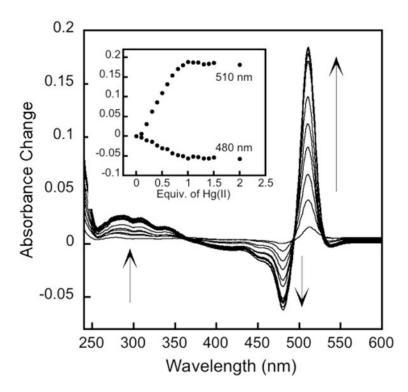
Figure 4.
Difference spectra obtained from the addition of Hg(II) to a solution of MS2 at pH 11 (50 mM CABS, 100 mM KCl). The concentration of MS2 was 10 μM. Aliquots of 1 mM HgCl$_2$ in water were added to yield Hg(II) concentrations of 0, 1, 2, 3, 4, 5, 6, 7, 8, 9, 10, 11, 12, 13, 14, 15, and 20 μM. Absorption increases occur at ca. 300 and 510 nm, and a decrease occurs at 480 nm upon Hg(II) coordination. Inset: Absorption change versus equiv. of Hg(II) in solution for MS2, which indicates formation of a 1:1 MS2:Hg(II) complex.
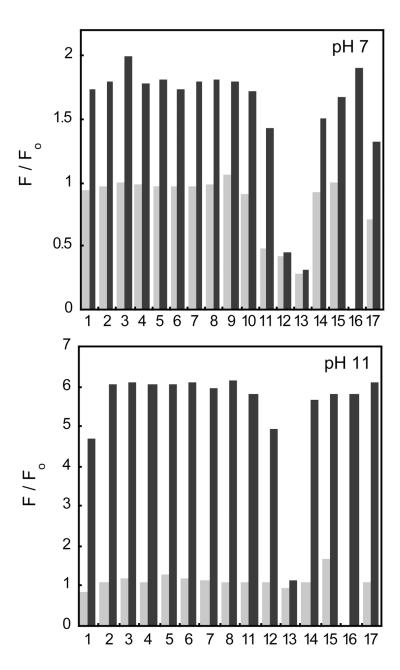
Figure 5.
Metal ion selectivity of MS3 at pH 7 (50 mM PIPES, 100 mM KCl) and pH 11 (50 mM CABS, 100 mM KCl). The light bars represent the fluorescence emission of a solution of MS3 and 67 equiv of the cation of interest: **1**, Li(I); **2**, Na(I); **3**, Rb(I); **4**, Mg(II); **5**, Ca(II); **6**, Sr(II); **7**, Ba (II); **8**, Cr(III); **9**, Mn(II); **10**, Fe(II); **11**, Co(II); **12**, Ni(II); **13**, Cu(II); **14**, Zn(II); **15**, Cd(II); **16**, Hg(II); **17**, Pb(II). The dark bars show the fluorescence change that occurs upon addition of 67 equiv of Hg(II) to the solution containing MS3 and the cation. The concentration of MS3 was 1 μM and excitation was provided at 500 nm. The response (F) is normalized with respect to the emission of the free dye (F_o). See Figure S5 of Supporting Information for MS2 data. The positive fluorescence response of MS2 and MS3 to Hg(II) also occur in the presence of millimolar concentrations of Li(I), Na(I), Rb(I), Mg(II), Ca(II), Sr(II) and Ba(II) (data not shown).

Scheme 1.

Table 1

Spectroscopic and Thermodynamic Data for Fluorescein-Based MS Sensors

	pH	Absorption λ (nm), $\varepsilon \times 10^4$ ($M^{-1}cm^{-1}$)		Emission λ (nm), Φ^a		$pK_a{}^b$	$EC_{50}{}^c$ (μM)
		Unbound	Hg(II)	Unbound	Hg(II)		
MS1[d]	7	505, 6.1	501, 7.3	524, 0.04	528. 0.11	7.1	0.410
MS2	7	500, 6.2	505, 6.9	526, 0.28	531, 0.27	8.0	
	9	502, 6.3	505, 8.2	526, 0.10	531, 0.28		
	11	504, 6.1	507, 7.8	526, 0.07	531, 0.24		0.384
MS3	7	501, 5.1	507, 5.9	526, 0.27	531, 0.28	8.2	
	11	504, 5.5	507, 6.4	525, 0.10	531, 0.26		1.6

[a] Fluorescein ($\Phi = 0.95$ in 0.1 N NaOH, ref. [56]) was used as the standard for the quantum yield measurements.

[b] The pK_a value of the aniline (MS1) or tertiary (MS2, MS3) nitrogen atom. This pK_a corresponds to a fluorescence increase when moving from high to low pH.

[c] The EC_{50} is the concentration of Hg(II) required to achieve 50% of the maximum fluorescence increase with 1 μM sensor.

[d] Data for MS1 were taken from ref. [49].